The Astrophysical Journal Supplement Series, 146:443–457, 2003 June

IONIZATION FRACTIONS OF SLOW IONS IN A PLASMA WITH KAPPA DISTRIBUTIONS FOR THE ELECTRON VELOCITY

S. Wannawichian, D. Ruffolo, and Yu. Yu. Kartavykh[1]
Department of Physics, Chulalongkorn University, Bangkok 10330, Thailand;
ramona@astro.phys.sc.chula.ac.th, david@astro.phys.sc.chula.ac.th, julia@astro.phys.sc.chula.ac.th
Received 2002 February 15; accepted 2002 December 23

ABSTRACT

The interpretation of a wide variety of astrophysical observations requires an understanding of how ionization fractions depend on plasma parameters. Observations have indicated that electron velocity distributions in space plasmas generally have enhanced high-energy tails. Instead of a Maxwellian distribution, they are better described by a kappa distribution, characterized by the kinetic temperature, T, and a parameter, κ, that quantifies the deviation from a Maxwellian. We calculate and tabulate the equilibrium ionization fractions of N, O, Ne, Mg, S, Si, Ar, Ca, Fe, and Ni, based on a balance of ionization and recombination processes, for 10^4 K $\leq T \leq 10^8$ K (or up to 10^9 K for Fe and Ni) and for various Maxwellian and kappa distributions. For a Maxwellian distribution of electrons, the mean charge as a function of temperature is characterized by plateaux corresponding to closed-shell charge states, with transitions over narrow ranges of $\log T$. However, for kappa distributions, which are more realistic models of the observed electron distributions in coronal or space plasmas, those transitions are substantially broader. We find that a lower κ value (more suprathermal electrons) frequently leads to a higher mean charge, especially for low temperatures, but can also lead to a lower mean charge in certain temperature ranges; these effects are associated with the sharp energy thresholds and resonances of ionization and dielectronic recombination cross sections, respectively. The results provide information for various applications in which observed ionization fractions are used as diagnostics of astrophysical plasmas.

Subject headings: atomic data — atomic processes — plasmas

On-line material: machine-readable table

1. INTRODUCTION

There is a wide range of applications in astrophysics and fusion research for calculations of ionization fractions and mean charges of various elements in hot plasmas. The observed ionization fractions, or the presence of a given ion, is frequently used as a diagnostic of the source plasma (e.g., of its temperature), especially in extreme ultraviolet or X-ray spectroscopy (e.g., Gallagher et al. 2001; Smith et al. 2001). Examples of astrophysical applications include solar physics topics, such as the corona, active regions, jets, flares, the FIP effect, CMEs, and the solar wind (e.g., Esser & Edgar 2000; Brosius 2001; Roussev et al. 2001). Charge state observations are used to indicate conditions at other stars or stellar-mass objects, including their coronae, jets, accretion shocks, accreting black holes, and supernova remnants (e.g., Drake et al. 2001; Huenemoerder, Canizares, & Schulz 2001; Wu, Cropper, & Ramsay 2001), and in the interstellar medium (e.g., Blair et al. 2000; Danforth, Blair, & Raymond 2001). There are further applications about galaxies and active galactic nuclei, jets, quasars (e.g., Fang et al. 2001; Hicks & Canizares 2001), and intercluster mediums (e.g., Reynolds, Heinz, & Begelman 2001). Ionization state observations are also used to study the intergalactic medium, shocks between galaxies, and cosmology (e.g., Fang & Canizares 2000). Furthermore, in fusion experiments, ionization fractions are used to study thermonuclear and magnetically confined fusion plasmas (e.g., May et al. 2000). Note that most of these applications require knowledge of the temperature dependence of ionization fractions, not only the mean charge.

Although there are several recent, useful tabulations of ionization fractions of various elements in a plasma (e.g., Arnaud & Rothenflug 1985; Arnaud & Raymond 1992; Mazzotta et al. 1998), these are based on the assumption that the electron velocity follows a Maxwellian distribution. However, that distribution would seem to be the exception, rather than the rule, for astrophysical plasmas (Collier 1999). Direct measurements of electron distributions in the solar wind, planetary magnetospheres, and other space plasmas show that the number of electrons at high energy is much greater than that for a Maxwellian distribution (e.g., Montgomery, Bame, & Hundhausen 1968; Feldman et al. 1975; Owocki & Scudder 1983; Maksimovic, Pierrard, & Riley 1997). Enhanced suprathermal tails have also been inferred in the solar corona, solar transition region, and radio sources inside and outside our solar system (Roussel-Dupré 1980; Shoub 1983; Owocki & Scudder 1983; Owocki & Canfield 1986; Maksimovic et al. 1997). In other words, astrophysical plasmas are rarely in thermal equilibrium. Therefore, the goal of the present work is to explore and tabulate how ionization fractions are affected by electron distributions with enhanced suprathermal tails.

One distribution that provides a suitable parameterization of observed data is the kappa distribution,

$$f_\kappa(E) = \frac{2\sqrt{E}}{\sqrt{\pi}(k_{\rm B}T)^{3/2}} A_\kappa \Big/ \left[1 + \frac{E}{(\kappa - 3/2)k_{\rm B}T}\right]^{\kappa+1}, \qquad (\kappa > 3/2)\ , \tag{1}$$

[1] Present address: Ioffe Physical-Technical Institute, Politekhnicheskaya 26, St. Petersburg 194021, Russia.

which is characterized by the kinetic temperature, T, and a parameter, κ, and where $A_\kappa \equiv \Gamma(\kappa+1)/[(\kappa-3/2)^{3/2}\Gamma(\kappa-1/2)]$, and k_B is the Boltzmann constant (Olbert et al. 1967; Olbert 1969). The kappa distribution (sometimes called a generalized Lorentzian) is a convenient and widely used analytic form that closely represents the nearly Maxwellian distribution of the low-energy "core," while the parameter κ controls the power-law form of the high-energy "tail." Note that as $\kappa \to \infty$, the distribution becomes Maxwellian, while a lower κ value implies a more enhanced and harder power-law tail. More specifically, for $E \gg k_B T$, we have $f_\kappa(E) \propto E^{-(\kappa+1/2)}$, while the speed distribution is $f_\kappa(v) \propto E^{-\kappa}$. Thus, reducing κ makes the distribution more non-Maxwellian. Indeed, at a fixed kinetic temperature, T, which fixes the mean energy or second moment of the velocity distribution, the enhanced, power-law tail at high energy is balanced by a redistribution at lower velocity as well. The overall effect is that a lower κ value gives an enhanced electron distribution at low speeds, a depressed distribution at medium speeds (for E of a few times $k_B T$), and an enhanced, power-law tail at high energy (see Fig. 1 of Owocki & Scudder 1983).

It has been suggested that non-Maxwellian distributions with enhanced high-energy tails may occur as an effect of the Rutherford cross section for the plasma electrons scattering off the background plasma (Scudder & Olbert 1979a; Scudder & Olbert 1979b), high gradients of particle concentration or temperature (Roussel-Dupré 1980; Shoub 1983; Owocki & Scudder 1983), velocity-space diffusion due to a suprathermal radiation field (Hasegawa, Mima, & Duong-van 1985), or wave-particle interactions (e.g., Ma & Summers 1998; see also corrections in Ma & Summers 1999a, 1999b). For observed data, various values of κ have been obtained from fits to electron distributions in space plasmas. For example, Pierrard, Maksimovic, & Lemaire (1999) found $\kappa \simeq 3.1$ and $\kappa \simeq 2$ for the slow and high-speed solar wind, respectively. Furthermore, Maksimovic et al. (1997) have fitted the kappa function to 16,000 electron velocity distributions measured in the solar wind by the electron plasma instrument on board the *Ulysses* spacecraft. These authors then derive κ values of $\simeq$2.71 and $\simeq$1.90 for the coronal source plasmas of the slow and fast wind, respectively.

Previous calculations of ionization fractions have been performed for a Maxwellian distribution of the plasma electron velocity (e.g., Arnaud & Rothenflug 1985; Arnaud & Raymond 1992; Mazzotta et al. 1998). For kappa distributions, the seminal work of Owocki & Scudder (1983) examined the ionization ratios O^{+6}/O^{+7} and Fe^{+11}/Fe^{+12}; Dzifčáková (1992) has calculated ionization fractions for Fe; and Luhn & Hovestadt (1985) and Ko et al. (1996) presented mean charges for various elements (useful for specialized applications regarding the solar wind and solar energetic particles). To our knowledge, the present work is the first to present ionization fractions of multiple elements for kappa distributions. We also demonstrate consistency with existing calculations for a Maxwellian distribution.

The ionization reactions considered here include direct ionization and excitation-autoionization (Arnaud & Rothenflug 1985; Arnaud & Raymond 1992; Sampson & Golden 1981). In addition, radiative recombination (Shull & Van Steenberg 1982a) and dielectronic recombination (Mazzotta et al. 1998) reactions are considered. In this case ions are taken to be slow, or essentially at rest with respect to the typical electron speed, which is often the case in their source plasma because of their much greater mass.

We only consider two-body collisions with plasma electrons, and we neglect collisions with other plasma ions, because the relative speed between two thermal ions is typically below the ionization threshold; such collisions would be important in a calculation of ionization fractions for high-speed ions (Kocharov et al. 2000; Ostryakov et al. 2000; Kartavykh et al. 2002). Furthermore, we only consider processes involving the ground states of ions. This assumption is appropriate for low-density plasmas in which the lifetime of excited states is smaller than the mean collision time, as pointed out by Arnaud & Raymond (1992), or even in higher density plasmas where the radiation field is not in equilibrium with the plasma, as in the case of the solar corona.

2. CALCULATION PROCEDURE

In this section, we present the procedure for calculating ionization and recombination rate coefficients assuming kappa distributions for the electron velocity, and deriving equilibrium ionization fractions and mean charges. The overall procedure is outlined in Figure 1. It is most instructive to start by explaining the desired final results (equilibrium ionization fractions and mean charges) and then to describe the steps needed to get there.

The main goal of this work is to calculate equilibrium ionization fractions, for applications as described in § 1. The equilibrium mean charge is simply the mean charge as weighted by the equilibrium ionization fractions. Naturally, the mean charge has much less information content, but it does provide a useful summary of how kappa distributions affect the ionization fractions, and indeed some observational work directly reports the mean charge.

The rate of change of n_q, the number density of ions of charge q, is given by

$$\frac{dn_q}{dt} = n_e[n_{q-1}S_{q-1} - n_q(S_q + \alpha_q) + n_{q+1}\alpha_{q+1}] \tag{2}$$

for $q = 0, \ldots, Z$, where S_q and α_q are temperature- and κ-dependent rate coefficients (in cm^3 s^{-1}) of ionization from charge q to $q+1$ and recombination from q to $q-1$, respectively. In equilibrium, we have $dn_q/dt = 0$ and

$$n_q S_q = n_{q+1}\alpha_{q+1}, \text{ for } q = 0, \ldots, Z-1 . \tag{3}$$

Therefore, the equilibrium ionization fractions ($n_q/n_{\rm tot}$, where $n_{\rm tot}$ is the total density of all charge states) can be immediately determined from the ionization and recombination rate coefficients.

Now comes the complicated part: calculating rate coefficients for the case of kappa distributions. We find it convenient to consider κ values that are integers, in which case most of the integrals can be performed analytically; for noninteger values, those integrals would instead be evaluated numerically. First, consider the case of ionization rate coefficients (starting at the

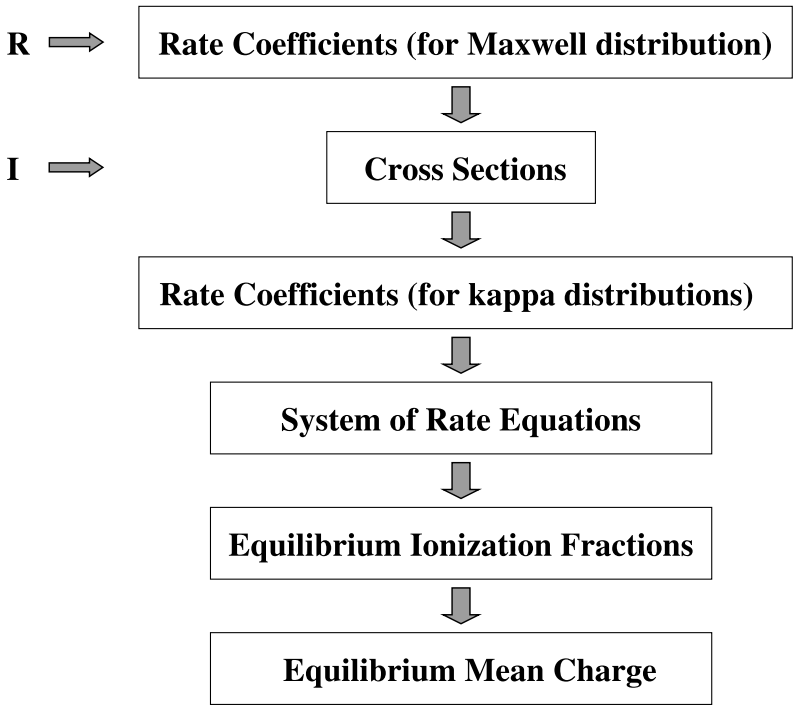

FIG. 1.—Calculation procedure for each element. The procedure starts at "R" for recombination rates and at "I" for ionization cross sections obtained from the literature (see text for details).

point indicated by "I" in Fig. 1). Cross section formulae for direct ionization and excitation-autoionization are available in the literature for all charge states of various elements (Arnaud & Rothenflug 1985; Arnaud & Raymond 1992; Sampson & Golden 1981). From these, we can derive ionization rate coefficients by integrating over the electron velocity distribution function:

$$S = \int v\sigma_I(v) f_\kappa(v) dv \; . \tag{4}$$

The cross section formulae and corresponding rate coefficient expressions are shown in §§ 2.1 and 2.2.

For recombination processes, the procedure has one extra step. The most recent results in the literature have not presented cross section formulae, but rather recombination rate coefficients under the assumption of a Maxwellian distribution for the electron velocity. Therefore, for recombination processes we start at point "R" in Figure 1: we first need to convert the rate coefficients provided in the literature (for the Maxwell distribution) to cross sections as a function of collision velocity (i.e., the electron velocity, since we are considering the case of slow ions). For dielectronic recombination, we use the rate coefficients (for Maxwell distributions) provided by Mazzotta et al. (1998). Note, however, that in some references, rate coefficients are expressed in a form that is apparently not related to a cross section formula. Thus, we cannot make use of the ionization rate coefficients of Voronov (1997). Similarly, we do not use the radiative recombination rate coefficients presented by Arnaud & Raymond (1992) or Verner & Ferland (1996) (which were in turn used by Mazzotta et al. 1998); instead, we use those of Shull & Van Steenberg (1982a). Nevertheless, our ionization fractions in the limit of a Maxwellian distribution are very similar to those of Arnaud & Raymond (1992) and Mazzotta et al. (1998) (see § 3.2).

After deriving the recombination cross sections, we can integrate over a kappa distribution for the electron velocity to obtain the desired rate coefficients:

$$\alpha = \int v\sigma_R(v) f_\kappa(v) dv \; . \tag{5}$$

The cross section and rate coefficient formulae for recombination processes are shown in §§ 2.3 and 2.4. Throughout this section, quantities of energy are to be expressed in eV, and constants taken from the literature refer to the numerical values (without units) unless otherwise indicated. Finally, some specialized numerical techniques are described in § 2.5.

2.1. *Direct Ionization*

Direct ionization (DI) is a process that can take place after the collision between a free electron and ion, in which an electron in the ion is directly excited to become another free electron. For direct ionization, the following cross section formula was introduced by Younger (1981). This form has been widely used, e.g., by Arnaud & Rothenflug (1985), Arnaud & Raymond

(1992), and Mazzotta et al. (1998):

$$\sigma_{\rm DI}(E) = \sum_j \frac{1}{uI_j^2}\left[A_j\left(1-\frac{1}{u}\right) + B_j\left(1-\frac{1}{u}\right)^2 + C_j\ln(u) + D_j\frac{\ln(u)}{u}\right] \times 10^{-14}\ {\rm cm}^2\ , \tag{6}$$

where for a level j, $u = E/I_j$, E is the energy of the incident electron, and I_j is the ionization potential. In this and all other ionization cross sections, we take the contribution of a level j to be zero for $u < 1$, i.e., below threshold. Here the constants A_j, B_j, C_j, and D_j for most ions are taken from Arnaud & Rothenflug (1985). Only for Fe ions are the constants taken from Arnaud & Raymond (1992).

For a kappa distribution we obtain the rate coefficient

$$\begin{aligned} S_{\rm DI}(T) = A_\kappa \frac{6.69\times10^{-7}}{(k_{\rm B}T)^{3/2}} \sum_j \Bigg\{ & A_j\left[\frac{(1+y)^{-\kappa}}{y\kappa} + \sum_{n=1}^{\kappa}\frac{1}{n(1+y)^n}\right] \\ & + B_j\left[\frac{(1+y)^{-\kappa}}{y\kappa} - (2+\kappa y+y)\ln\frac{1+y}{y} + \sum_{n=1}^{\kappa}\frac{\kappa y - ny + y + 2}{n(1+y)^n} + 1\right] \\ & + \frac{C_j}{y\kappa}\left[\ln\left(\frac{1+y}{y}\right) - \sum_{n=1}^{\kappa-1}\frac{1}{n(1+y)^n}\right] + D_j\int_1^\infty \frac{\ln(u)}{u(1+yu)^{\kappa+1}}\,du\Bigg\}\ {\rm cm}^3\ {\rm s}^{-1}\ , \end{aligned} \tag{7}$$

where $y = I_j/[k_{\rm B}T(\kappa - 3/2)]$. The last term cannot be calculated analytically; therefore, numerical integration is necessary.

2.2. *Excitation-Autoionization*

Excitation-autoionization (EA) takes place by a process similar to the direct ionization process. However, in this case an electron in an inner shell is excited. With its high binding energy, the excitation energy may be insufficient to ionize the inner shell electron, which just releases the excitation energy and comes back to the ground state. Then a different, outer shell electron can receive that energy and become another free electron. Following the advice of various articles in the literature, an excitation-autoionization cross section ($\sigma_{\rm EA}$) is used for certain ions. In particular, there are suggested forms for selected multielectron Fe ions, for the ions Ca^{+0} and Ca^{+1}, and for (non-Fe) ions of various sequences; in all other cases, $\sigma_{\rm EA}$ is neglected in comparison with $\sigma_{\rm DI}$. A sequence is defined by the number of remaining electrons, e.g., the lithium sequence refers to ions with three remaining electrons, so ions in the same sequence have a similar ground state electronic configuration.

2.2.1. *Selected* Fe *Ions*

For selected multielectron Fe ions, the EA cross sections are calculated by the following formula (Arnaud & Raymond 1992):

$$\sigma_{\rm EA}(u) = \frac{1}{uI_{\rm EA}}\left[A + B\left(1-\frac{1}{u}\right) + C\left(1-\frac{1}{u^2}\right) + D\left(1-\frac{1}{u^3}\right) + F\ln(u)\right] \times 10^{-16}\ {\rm cm}^2\ , \tag{8}$$

where $u = E/I_{\rm EA}$, E is the incident electron energy, $I_{\rm EA}$ is the EA threshold energy, and A, B, C, D, and F are constants taken from a table of Arnaud & Raymond (1992). Note that these authors use nonzero constants only for Fe^{+2} to Fe^{+15} and for Fe^{+23}.

For kappa distributions, the rate coefficient is

$$\begin{aligned} S_{\rm EA}(T) = c\Bigg\{ & A\frac{(1+y)^{-\kappa}}{y\kappa} + B\left[\frac{(1+y)^{-\kappa}}{y\kappa} - \ln\left(\frac{1+y}{y}\right) + \sum_{n=1}^{\kappa}\frac{1}{n(1+y)^n}\right] \\ & + C\left[\frac{(1+y)^{-\kappa}}{y\kappa} - y\sum_{n=1}^{\kappa}\frac{\kappa-n+1}{n(1+y)^n} + (\kappa+1)y\ln\left(\frac{1+y}{y}\right) - 1\right] \\ & + D\left[\sum_{n=1}^{\kappa}\frac{(\kappa-n+1)(\kappa-n+2)y^2}{2n(1+y)^n} - \frac{(\kappa+1)(\kappa+2)}{2}y^2\ln\left(\frac{1+y}{y}\right) + \frac{(1+y)^{-\kappa}}{y\kappa} + (\kappa+1)y - \frac{1}{2}\right] \\ & + \frac{F}{y\kappa}\left[\ln\left(\frac{1+y}{y}\right) - \sum_{n=1}^{\kappa-1}\frac{1}{n(1+y)^n}\right]\Bigg\}\ {\rm cm}^3\ {\rm s}^{-1}\ , \end{aligned} \tag{9}$$

where

$$y = \frac{I_{\rm EA}}{(\kappa-3/2)k_{\rm B}T}, \quad c = \frac{6.69\times10^{-9}A_\kappa}{(k_{\rm B}T)^{3/2}}\ . \tag{10}$$

2.2.2. Ca^{+0} *and* Ca^{+1}

For Ca^{+0} and Ca^{+1}, EA cross sections are from Arnaud & Rothenflug (1985):

$$\sigma_{\rm EA}(u) = \frac{a}{u}[1 + b\ln(u)]\ {\rm cm}^2\ , \tag{11}$$

where $u = E/I_{\rm EA}$.

For Ca^{+0}: $a = 6.0 \times 10^{-17}$ cm^2; $b = 1.12$; $I_{\rm EA} = 25$ eV. For Ca^{+1}: $a = 9.8 \times 10^{-17}$ cm^2; $b = 1.12$; $I_{\rm EA} = 29$ eV.

For a kappa distribution, the rate coefficient becomes

$$S_{\rm EA}(T) = \frac{6.69 \times 10^7}{(k_{\rm B}T)^{3/2}} A_\kappa I_{\rm EA}^2 a \left\{ \frac{(1+y)^{-\kappa}}{\kappa y} + \frac{b}{\kappa y}\left[\ln\left(\frac{1+y}{y}\right) - \sum_{n=1}^{\kappa-1} \frac{1}{n(1+y)^n}\right]\right\}\ {\rm cm}^3\ {\rm s}^{-1}\ , \tag{12}$$

for y defined as in equation (10).

2.2.3. Li *Sequence*

In the case of the lithium sequence (i.e., ions with three electrons, N^{+4}, O^{+5}, Ne^{+7}, etc.) the cross section formula for excitation-autoionization is (Sampson & Golden 1981)

$$\sigma_{\rm EA}(u) = \frac{2\pi a_0^2}{I_{2s} Z_{\rm eff}^2(1s) u} \beta H(u - \xi_2)\left[Z^2\Omega_H(1 \to 2)\right]_{\rm eff}\ , \tag{13}$$

where

$$\begin{aligned}
\left[Z^2\Omega_H(1 \to 2)\right]_{\rm eff} &= 2.220\ln(u) + 0.669\left(1 - \frac{1}{u}\right) + \frac{0.488}{u} + \frac{1.201}{u^2}\ {\rm eV}\ , \\
H(x) &= \begin{cases} 0\ , & \text{if } x < 0\ ; \\ 1\ , & \text{if } x > 0\ , \end{cases} \\
\xi_2 &= \frac{I_{\rm EA}}{I_{2s}}\ , \\
I_{2s} &= \frac{13.6}{4}(Z - 1.679)^2\ {\rm eV}\ , \\
I_{\rm EA} &= 13.6\left[(Z - 0.835)^2 - \frac{1}{4}(Z - 1.620)^2\right]\ {\rm eV}\ , \\
Z_{\rm eff}(1s) &= Z - 0.43\ , \\
u &= \frac{E}{I_{2s}}\ , \\
\beta &= \frac{1}{1 + 2 \times 10^{-4} Z^3}\ , \\
a_0 &= \text{Bohr radius} = 5.292 \times 10^{-9}\ {\rm cm}\ .
\end{aligned}$$

where Z is the nuclear charge. Note that $u - \xi_2$, the argument of the step function, H, is the difference between the impact electron energy and the threshold energy for the transition.

For a kappa distribution, the rate coefficient is

$$\begin{aligned}
S_{\rm EA}(T) = c\Bigg\{ & \frac{2.220}{\kappa y}\left[\frac{\ln\xi_2}{(1+y\xi_2)^\kappa} - \ln\left(\frac{1+y\xi_2}{y\xi_2}\right) - \sum_{n=1}^{\kappa-1}\frac{1}{n(1+y\xi_2)^n}\right] \\
& + 0.669\left[-\ln\left(\frac{1+y\xi_2}{y\xi_2}\right) + \frac{(1+y\xi_2)^{-\kappa}}{y\kappa} + \sum_{n=1}^{\kappa}\frac{1}{n(1+y\xi_2)^n}\right] \\
& + 0.488\left[\ln\left(\frac{1+y\xi_2}{y\xi_2}\right) - \sum_{n=1}^{\kappa}\frac{1}{n(1+y\xi_2)^n}\right] \\
& + 1.201\left[\frac{1}{\xi_2} - (\kappa+1)y\ln\left(\frac{1+y\xi_2}{y\xi_2}\right) + \sum_{n=1}^{\kappa}\frac{(\kappa-n+1)y}{n(1+y\xi_2)^n}\right]\Bigg\}\ {\rm cm}^3\ {\rm s}^{-1}\ ,
\end{aligned} \tag{14}$$

where

$$c = \frac{4.20 \times 10^8 A_\kappa}{(k_{\rm B}T)^{3/2}} \frac{\beta(a_0/{\rm cm})^2}{Z_{\rm eff}^2(1s)} I_{2s}, \quad y = \frac{I_{2s}}{(\kappa - 3/2)k_{\rm B}T}\ . \tag{15}$$

2.2.4. Na *Sequence* ($Z \leq 16$)

We use the EA cross section from Arnaud & Rothenflug (1985) when considering ions of the sodium sequence with atomic number $Z \leq 16$:

$$\sigma_{\rm EA}(u) = \frac{a}{u}\left(1 - \frac{1}{u}\right) \ {\rm cm}^2 \ , \tag{16}$$

where $u = E/I_{\rm EA}$, $I_{\rm EA} = 26(Z-10)$ eV, and $a = 2.8 \times 10^{-17}(Z-11)^{-0.7}$.

The rate coefficient for kappa distributions is

$$S_{\rm EA}(T) = \frac{6.69 \times 10^7}{(k_{\rm B}T)^{3/2}} A_\kappa I_{\rm EA}^2 a \left[\frac{(1+y)^{-\kappa}}{\kappa y} - \ln\left(\frac{1+y}{y}\right) + \sum_{n=1}^{\kappa} \frac{1}{n(1+y)^n}\right] \ {\rm cm}^3 \ {\rm s}^{-1} \ , \tag{17}$$

where

$$y = \frac{I_{\rm EA}}{(\kappa - 3/2)k_{\rm B}T} \ . \tag{18}$$

2.2.5. Na *Sequence* ($18 \leq Z \leq 28$)

For ions of the sodium sequence, in the range $18 \leq Z \leq 28$, we use the EA cross section of Arnaud & Rothenflug (1985):

$$\sigma_{\rm EA}(u) = \frac{a}{u}\left(1 - \frac{1}{u^3}\right) \ {\rm cm}^2 \ , \tag{19}$$

where $u = E/I_{\rm EA}$, $I_{\rm EA} = 11(Z-10)^{1.5}$ eV, and $a = 1.3 \times 10^{-14}(Z-10)^{-3.73}$.

For kappa distributions, the rate coefficient is

$$S_{\rm EA}(T) = c\left[\frac{(1+y)^{-\kappa}}{\kappa y} + (\kappa+1)y - \frac{1}{2}(\kappa+1)(\kappa+2)y^2 \ln\left(\frac{1+y}{y}\right) + \sum_{n=1}^{\kappa} \frac{(\kappa-n+1)(\kappa-n+2)y^2}{2n(1+y)^n} - \frac{1}{2}\right] \ {\rm cm}^3 \ {\rm s}^{-1} \ , \tag{20}$$

where

$$y = \frac{I_{\rm EA}}{(\kappa - 3/2)k_{\rm B}T}, \quad c = \frac{6.69 \times 10^7}{(k_{\rm B}T)^{3/2}} A_\kappa I_{\rm EA}^2 a \ . \tag{21}$$

2.2.6. Mg *to* Ar *Sequences*

For sequences from magnesium to argon, the EA cross section of Arnaud & Rothenflug (1985) can be calculated as follows:

$$\sigma_{\rm EA}(u) = \frac{a}{u}\left(1 - \frac{1}{u^3}\right) \ {\rm cm}^2 \ , \tag{22}$$

where $u = E/I_{\rm EA}$, $aI_{\rm EA} = 4 \times 10^{-13}Z^{-2}$, and

$$I_{\rm EA} = \begin{cases} 10.3(Z-10)^{1.52} \ {\rm eV}, & {\rm Mg\ sequence\ ;} \\ 18.0(Z-11)^{1.33} \ {\rm eV}, & {\rm Al\ sequence\ ;} \\ 18.4(Z-12)^{1.36} \ {\rm eV}, & {\rm Si\ sequence\ ;} \\ 23.7(Z-13)^{1.29} \ {\rm eV}, & {\rm P\ sequence\ ;} \\ 40.1(Z-14)^{1.10} \ {\rm eV}, & {\rm S\ sequence\ .} \end{cases} \tag{23}$$

The rate coefficient for the case of a kappa distribution is

$$S_{\rm EA}(T) = c\left[\frac{(1+y)^{-\kappa}}{\kappa y} + (\kappa+1)y - \frac{1}{2}(\kappa+1)(\kappa+2)y^2 \ln\left(\frac{1+y}{y}\right) + \sum_{n=1}^{\kappa} \frac{(\kappa-n+1)(\kappa-n+2)y^2}{2n(1+y)^n} - \frac{1}{2}\right] \ {\rm cm}^3 \ {\rm s}^{-1} \ , \tag{24}$$

where

$$y = \frac{I_{\rm EA}}{(\kappa - 3/2)k_{\rm B}T}, \quad c = \frac{6.69 \times 10^7}{(k_{\rm B}T)^{3/2}} A_\kappa I_{\rm EA}^2 a \ . \tag{25}$$

2.3. *Radiative Recombination*

Radiative recombination (RR) is the process whereby a free electron is bound to the ion after the collision. The electron emits its excess energy in the form of electromagnetic radiation.

For all elements, the radiative recombination cross section is related to the rate coefficient (for a Maxwellian distribution) from Shull & Van Steenberg (1982a). Those authors specify the rate coefficient formula:

$$\alpha_{\rm RR}(T) = A_{\rm rad}(T/10^4\ {\rm K})^{-\eta}\ {\rm cm}^3\ {\rm s}^{-1}\ , \tag{26}$$

where the coefficients $A_{\rm rad}$ and η are presented in Table 2 of that paper. We have corrected their tabulated values according to their published errata (Shull & Van Steenberg 1982b), and an apparent misprint in the value of $A_{\rm rad}$ for recombination from Ca^{+11} to Ca^{+10} as pointed out by Arnaud & Rothenflug (1985). The corresponding cross section has the form of a power law (Luhn & Hovestadt 1987):

$$\sigma_{\rm RR}(E) = \frac{1.495\times10^{-8}}{\Gamma(3/2-\eta)}\frac{(k_{\rm B})^{\eta}}{(10^4\ {\rm K})^{-\eta}}A_{\rm rad}E^{-(\eta+1/2)}\ {\rm cm}^2\ . \tag{27}$$

For a kappa distribution, the rate coefficient is

$$\alpha_{\rm RR}(T) = A_{\rm rad}A_{\kappa}\frac{\Gamma(\kappa+\eta-1/2)}{\Gamma(\kappa+1)}\frac{(\kappa-3/2)^{-\eta+3/2}}{T^{\eta}(10^4\ {\rm K})^{-\eta}}\ {\rm cm}^3\ {\rm s}^{-1}\ . \tag{28}$$

2.4. *Dielectronic Recombination*

Dielectronic recombination (DR) is more complicated than the previous process. After the collision, the initially free electron becomes bound and releases its energy, which is taken up by the excitation of another, bound electron. Thus, this is a resonant process, taking place for specific values of the incoming electron energy. The excited electron comes back to the ground state by emitting energy through electromagnetic radiation. Finally, the ion has gained one electron. According to Mazzotta et al. (1998), the same dielectronic recombination rate coefficient formula can be used for all elements. For a Maxwellian distribution, that formula is

$$\alpha_{\rm DR}(E) = \frac{1}{(k_{\rm B}T)^{3/2}}\sum_{j=1}^{4}c_j\exp\left(-\frac{E_j}{k_{\rm B}T}\right)\ {\rm cm}^3\ {\rm s}^{-1}\ . \tag{29}$$

Each term in the sum corresponds to a different dielectronic transition. The coefficients c_j and E_j for each ion are tabulated by Mazzotta et al. (1998). This rate coefficient corresponds to a cross section that is a sum of delta functions (Luhn & Hovestadt 1987):

$$\sigma_{\rm DR}(E) = 1.495\times10^{-8}\sum_{j=1}^{4}c_j\frac{\delta(E-E_j)}{E_j}\ {\rm cm}^2\ . \tag{30}$$

For a kappa distribution, the corresponding rate coefficient is

$$\alpha_{\rm DR}(T) = \frac{A_{\kappa}}{(k_{\rm B}T)^{3/2}}\sum_{j=1}^{4}c_j\left[1+\frac{E_j}{(\kappa-3/2)k_{\rm B}T}\right]^{-(\kappa+1)}\ {\rm cm}^3\ {\rm s}^{-1}\ . \tag{31}$$

2.5. *Numerical Techniques*

In the calculation procedure, numerical methods are used to integrate certain terms in the rate coefficients. A newly developed robust integration method is used to deal with the difficulty of integrating over an infinite domain (which, for example, causes problems in some commercial software packages). Fortunately, all integrands considered here exhibit a rise to a maximum value followed by a monotonic decline. The first step of our integration technique is to find a suitable upper limit of integration over the independent variable, say u. We use the bisection method to determine a sequence of increasing u-grid points, where the integrand reaches its maximum, half-maximum, quarter-maximum, etc. We integrate separately from the lower limit to the first u-grid point, from the first to the second, etc., using the two-interval Simpson's rule. The process was terminated when integrating to a further u-grid point changed the total integration result by less than a fractional tolerance of 10^{-4}. Finally, we improved the accuracy by increasing the number of intervals used for Simpson's rule (between u-grid points) in steps of 2 until the fractional change was less than 10^{-11}. This method was found to be efficient and sufficiently robust to accommodate the very wide range of κ and T values considered in this work.

TABLE 1

IONIZATION FRACTIONS FOR 10 SELECTED ELEMENTS AS A FUNCTION OF TEMPERATURE FOR VARIOUS KAPPA DISTRIBUTIONS AND A MAXWELLIAN DISTRIBUTION OF ELECTRON VELOCITY

Element	Z	κ[a]	log T (K)	$\langle Q \rangle$	+0	+1	+2	+3	+4	+5	+6	+7
N	7	3	4.0	1.756	2.471	0.483	0.239	1.047	2.964	9.999	9.999	9.999
N	7	3	4.1	1.994	2.926	0.712	0.209	0.740	2.370	4.966	9.999	9.999
N	7	3	4.2	2.225	3.375	0.977	0.240	0.515	1.882	4.150	9.999	9.999
N	7	3	4.3	2.437	3.799	1.259	0.315	0.368	1.505	3.441	9.999	9.999
N	7	3	4.4	2.622	4.168	1.528	0.417	0.281	1.211	2.818	9.999	9.999
N	7	3	4.5	2.786	4.516	1.796	0.529	0.236	0.989	2.269	9.999	9.999
N	7	3	4.6	2.946	4.830	2.044	0.650	0.224	0.814	1.769	9.999	9.999
N	7	3	4.7	3.139	9.999	2.302	0.792	0.242	0.673	1.310	4.927	9.999
N	7	3	4.8	3.414	9.999	2.604	0.975	0.304	0.575	0.889	4.186	9.999
N	7	3	4.9	3.802	9.999	2.980	1.233	0.436	0.543	0.542	3.516	9.999

NOTES.—For charge state q, the ionization fraction is tabulated as $-\log(n_q/n_{\rm tot})$, where $n_{\rm tot}$ is the total density of all charge states of that element. The value 9.999 indicates that $n_q < 10^{-5} n_{\rm tot}$. The full version of this table contains columns for charge states up to +28, to accommodate elements up to Ni. Table 1 is available in its entirety in the electronic edition of the *Astrophysical Journal Supplement*. A portion is shown here for guidance regarding its form and content.

[a] The letter " M " indicates a Maxwellian distribution.

3. RESULTS AND DISCUSSION

After determining the rate coefficients, we solved the equations for ionization equilibrium (eq. [3]) to obtain the ionization fractions and mean charges for various elements. We present them as a function of temperature and the κ value, including the limiting case of a Maxwellian distribution, in Table 1. The ionization fractions for N, O, Ne, Mg, Si, S, Ar, Ca, Fe, and Ni are tabulated for κ values of 3, 5, and 10 and a Maxwellian distribution. The temperature range is from 10^4 to 10^8 (for N to Ca) or to 10^9 K (for Fe and Ni). The ionization fraction of charge state q is presented in terms of $-\log(n_q/n_{\rm tot})$, where $n_{\rm tot}$ is the total density of all charge states of that element. The value 9.999 indicates that $n_q < 10^{-5} n_{\rm tot}$ for this ion. As examples, Tables 2A, 2B, 3A, and 3B are shown for Fe ions in the cases of Maxwellian and $\kappa = 5$ distributions for the electron velocity. In these tables, the symbols " *** " indicate that $-\log(n_q/n_{\rm tot})$ is greater than 5, i.e., $n_q < 10^{-5} n_{\rm tot}$.

TABLE 2A

IONIZATION FRACTIONS FOR Fe AS A FUNCTION OF TEMPERATURE FOR A MAXWELLIAN DISTRIBUTION OF ELECTRON VELOCITY: Fe^{+0}–Fe^{+13}

log T	Fe^{+0}	Fe^{+1}	Fe^{+2}	Fe^{+3}	Fe^{+4}	Fe^{+5}	Fe^{+6}	Fe^{+7}	Fe^{+8}	Fe^{+9}	Fe^{+10}	Fe^{+11}	Fe^{+12}	Fe^{+13}	$\langle Q \rangle$
4.0.....	0.916	0.056	4.000	***	***	***	***	***	***	***	***	***	***	***	0.879
4.1.....	1.454	0.019	2.166	***	***	***	***	***	***	***	***	***	***	***	0.972
4.2.....	1.978	0.085	0.778	***	***	***	***	***	***	***	***	***	***	***	1.156
4.3.....	2.883	0.588	0.131	***	***	***	***	***	***	***	***	***	***	***	1.739
4.4.....	3.921	1.292	0.023	3.058	***	***	***	***	***	***	***	***	***	***	1.950
4.5.....	4.718	1.750	0.022	1.506	***	***	***	***	***	***	***	***	***	***	2.013
4.6.....	***	2.149	0.157	0.528	3.813	***	***	***	***	***	***	***	***	***	2.289
4.7.....	***	2.691	0.507	0.170	1.968	***	***	***	***	***	***	***	***	***	2.696
4.8.....	***	3.250	0.901	0.126	0.901	3.640	***	***	***	***	***	***	***	***	2.999
4.9.....	***	3.876	1.370	0.281	0.378	1.840	***	***	***	***	***	***	***	***	3.405
5.0.....	***	4.632	1.980	0.613	0.223	0.833	3.046	***	***	***	***	***	***	***	3.884
5.1.....	***	***	2.700	1.098	0.322	0.371	1.809	4.081	***	***	***	***	***	***	4.373
5.2.....	***	***	3.524	1.697	0.581	0.208	1.023	2.491	4.933	***	***	***	***	***	4.798
5.3.....	***	***	4.418	2.383	0.971	0.251	0.542	1.403	3.054	***	***	***	***	***	5.253
5.4.....	***	***	***	3.191	1.521	0.504	0.350	0.720	1.741	***	***	***	***	***	5.851
5.5.....	***	***	***	4.174	2.269	0.984	0.441	0.395	0.900	4.000	***	***	***	***	6.540
5.6.....	***	***	***	***	3.183	1.657	0.767	0.361	0.434	2.657	***	***	***	***	7.156
5.7.....	***	***	***	***	4.176	2.432	1.232	0.511	0.215	1.712	3.472	***	***	***	7.583
5.8.....	***	***	***	***	***	3.250	1.768	0.762	0.147	1.047	2.162	3.579	***	***	7.896
5.9.....	***	***	***	***	***	4.119	2.380	1.117	0.219	0.615	1.201	2.050	3.208	***	8.313
6.0.....	***	***	***	***	***	***	3.167	1.663	0.513	0.495	0.640	1.007	1.661	2.932	9.144
6.1.....	***	***	***	***	***	***	4.295	2.572	1.189	0.812	0.574	0.528	0.747	1.496	10.476
6.2.....	***	***	***	***	***	***	***	3.859	2.265	1.569	1.012	0.609	0.450	0.749	11.846
6.3.....	***	***	***	***	***	***	***	***	3.771	2.798	1.949	1.240	0.748	0.655	13.618
6.4.....	***	***	***	***	***	***	***	***	***	4.489	3.375	2.393	1.603	1.161	15.030
6.5.....	***	***	***	***	***	***	***	***	***	***	4.907	3.680	2.619	1.870	15.574
6.6.....	***	***	***	***	***	***	***	***	***	***	***	4.920	3.615	2.584	15.858
6.7.....	***	***	***	***	***	***	***	***	***	***	***	***	4.578	3.303	16.168
6.8.....	***	***	***	***	***	***	***	***	***	***	***	***	4.330	2.987	16.574
6.9.....	***	***	***	***	***	***	***	***	***	***	***	***	***	3.943	17.863

TABLE 2B

IONIZATION FRACTIONS FOR Fe AS A FUNCTION OF TEMPERATURE FOR A MAXWELLIAN DISTRIBUTION OF ELECTRON VELOCITY: Fe^{+13}–Fe^{+26}

log T	Fe^{+13}	Fe^{+14}	Fe^{+15}	Fe^{+16}	Fe^{+17}	Fe^{+18}	Fe^{+29}	Fe^{+20}	Fe^{+21}	Fe^{+22}	Fe^{+23}	Fe^{+24}	Fe^{+25}	Fe^{+26}	$\langle Q \rangle$
6.0.....	2.932	4.433	***	***	***	***	***	***	***	***	***	***	***	***	9.144
6.1.....	1.496	2.411	3.616	4.350	***	***	***	***	***	***	***	***	***	***	10.476
6.2.....	0.749	1.159	1.816	2.160	***	***	***	***	***	***	***	***	***	***	11.846
6.3.....	0.655	0.616	0.820	0.868	3.304	***	***	***	***	***	***	***	***	***	13.618
6.4.....	1.161	0.733	0.557	0.364	2.176	4.414	***	***	***	***	***	***	***	***	15.030
6.5.....	1.870	1.098	0.607	0.204	1.512	3.130	4.797	***	***	***	***	***	***	***	15.574
6.6.....	2.584	1.512	0.753	0.160	1.047	2.158	3.275	4.863	***	***	***	***	***	***	15.858
6.7.....	3.303	1.961	0.965	0.194	0.719	1.405	2.041	3.154	4.454	***	***	***	***	***	16.168
6.8.....	2.987	1.738	0.902	0.390	0.602	0.918	1.201	1.909	2.780	3.849	***	***	***	***	16.574
6.9.....	3.943	2.488	1.451	0.748	0.679	0.683	0.641	1.005	1.512	2.178	3.101	4.200	***	***	17.863
7.0.....	***	3.620	2.387	1.494	1.168	0.888	0.560	0.619	0.810	1.137	1.710	2.450	***	***	19.485
7.1.....	***	***	3.658	2.584	2.027	1.496	0.915	0.703	0.616	0.642	0.913	1.357	***	***	21.016
7.2.....	***	***	***	3.932	3.162	2.398	1.584	1.130	0.793	0.554	0.556	0.754	3.830	***	22.223
7.3.....	***	***	***	***	4.397	3.419	2.394	1.720	1.160	0.686	0.459	0.453	2.844	***	22.935
7.4.....	***	***	***	***	***	4.473	3.249	2.370	1.604	0.912	0.473	0.297	2.139	4.493	23.331
7.5.....	***	***	***	***	***	***	4.076	3.008	2.049	1.165	0.544	0.215	1.597	3.466	23.572
7.6.....	***	***	***	***	***	***	4.874	3.627	2.498	1.434	0.639	0.180	1.173	2.631	23.758
7.7.....	***	***	***	***	***	***	***	4.238	2.940	1.708	0.762	0.184	0.851	1.965	23.947
7.8.....	***	***	***	***	***	***	***	4.840	3.386	2.003	0.919	0.227	0.620	1.444	24.170
7.9.....	***	***	***	***	***	***	***	***	3.850	2.323	1.107	0.312	0.470	1.042	24.432
8.0.....	***	***	***	***	***	***	***	***	4.333	2.676	1.345	0.443	0.387	0.741	24.724
8.1.....	***	***	***	***	***	***	***	***	4.817	3.033	1.595	0.604	0.365	0.533	24.990
8.2.....	***	***	***	***	***	***	***	***	***	3.431	1.874	0.793	0.383	0.386	25.223
8.3.....	***	***	***	***	***	***	***	***	***	3.773	2.145	0.980	0.431	0.287	25.397
8.4.....	***	***	***	***	***	***	***	***	***	4.131	2.415	1.172	0.488	0.219	25.528
8.5.....	***	***	***	***	***	***	***	***	***	4.464	2.673	1.358	0.554	0.171	25.627
8.6.....	***	***	***	***	***	***	***	***	***	4.780	2.917	1.535	0.625	0.135	25.701
8.7.....	***	***	***	***	***	***	***	***	***	***	3.148	1.703	0.694	0.109	25.756
8.8.....	***	***	***	***	***	***	***	***	***	***	3.364	1.856	0.759	0.091	25.797
8.9.....	***	***	***	***	***	***	***	***	***	***	3.559	1.999	0.822	0.076	25.829
9.0.....	***	***	***	***	***	***	***	***	***	***	3.748	2.137	0.883	0.065	25.854

In addition to ionization fractions, we have obtained the equilibrium mean charge for each element, $\langle Q \rangle$. This is a convenient quantity for summarizing direct measurements of ion populations, e.g., the solar wind (e.g., Gloeckler et al. 1999) or solar energetic particles (e.g., Möbius et al. 1999). For the latter, $\langle Q \rangle$ has frequently been interpreted as a proxy of the source plasma temperature. Here we view the mean charge as a convenient statistic for summarizing the effects of a suprathermal, power-law tail of the electron velocity distribution (as parameterized by the κ value) on the ionization balance of each element (Fig. 2). Such effects are described in § 3.1.

One way in which we have checked our formulae and calculations for kappa distributions is by calculating ionization fractions for large κ (here, $\kappa = 1000$), which should be similar to those for a Maxwellian distribution. This was verified to be the case for each element and each temperature, as shown in Figure 2. We have also confirmed that for cases where previous results are available, our calculations are similar to those of other authors, as seen in § 3.2. The magnitude of the differences between various calculations (Figs. 3 and 4) provides a measure of their uncertainty.

3.1. *Effects of a Kappa Distribution on Ionization Fractions and Mean Equilibrium Charges*

For a Maxwellian distribution of electrons, the mean charge as a function of temperature is characterized by plateaux corresponding to closed-shell charge states, with transitions over narrow ranges of log T. However, for kappa distributions, the low-temperature ionization fractions are greatly shifted to higher charge, so much so that some plateaux are washed out, while at high temperatures the transitions between plateaux are substantially broader in log T (see Fig. 2).

To understand the physical basis of these effects, we note that the effect of a kappa distribution (or since $\kappa \rightarrow \infty$ implies a Maxwellian, we may speak of the effect of a lower κ value) on ionization or dielectronic recombination (DR) rates depends on the threshold or resonance energy compared with $k_B T$ (Owocki & Scudder 1983), while the fractional effect on radiative recombination (RR) rates is temperature-independent for the power-law cross sections employed here (as there is no characteristic energy scale for a power law). For a given ionization or DR transition, at low temperatures reducing κ can greatly enhance the rate relative to that for a Maxwellian, because of the greatly enhanced suprathermal tail above threshold. As we noted in § 1, a lower κ value also gives an enhanced electron distribution at low speeds, and a depressed distribution at medium speeds. Thus, for $k_B T$ roughly on the order of the threshold or resonance energy the rate is slightly reduced, and at high temperatures the rate is again enhanced because there are more electrons at low v (though these represent much weaker fractional changes than that at low temperature). The matter is further complicated by the two recombination processes: for most of the effects described in this section, RR dominates over DR, so the strong enhancement of high-threshold processes mainly favors

TABLE 3A

IONIZATION FRACTIONS FOR Fe AS A FUNCTION OF TEMPERATURE FOR A KAPPA DISTRIBUTION OF ELECTRON VELOCITY, WITH $\kappa = 5$: Fe^{+0}–Fe^{+13}

log T	Fe^{+0}	Fe^{+1}	Fe^{+2}	Fe^{+3}	Fe^{+4}	Fe^{+5}	Fe^{+6}	Fe^{+7}	Fe^{+8}	Fe^{+9}	Fe^{+10}	Fe^{+11}	Fe^{+12}	Fe^{+13}	$\langle Q \rangle$
4.0.....	3.305	0.862	0.095	1.241	3.484	***	***	***	***	***	***	***	***	***	1.920
4.1.....	3.910	1.312	0.108	0.772	2.522	***	***	***	***	***	***	***	***	***	2.126
4.2.....	4.564	1.818	0.230	0.426	1.690	4.051	***	***	***	***	***	***	***	***	2.401
4.3.....	***	2.378	0.485	0.241	1.032	2.902	***	***	***	***	***	***	***	***	2.760
4.4.....	***	2.998	0.882	0.232	0.569	1.957	4.206	***	***	***	***	***	***	***	3.159
4.5.....	***	3.644	1.367	0.390	0.310	1.228	3.003	***	***	***	***	***	***	***	3.568
4.6.....	***	4.299	1.906	0.682	0.239	0.713	2.039	4.063	***	***	***	***	***	***	3.980
4.7.....	***	4.957	2.473	1.060	0.335	0.399	1.323	2.880	4.996	***	***	***	***	***	4.404
4.8.....	***	***	3.016	1.503	0.554	0.270	0.854	1.974	3.639	***	***	***	***	***	4.817
4.9.....	***	***	3.628	1.950	0.831	0.275	0.586	1.320	2.578	***	***	***	***	***	5.192
5.0.....	***	***	4.194	2.408	1.139	0.371	0.459	0.873	1.786	***	***	***	***	***	5.584
5.1.....	***	***	4.811	2.886	1.477	0.543	0.435	0.597	1.232	4.252	***	***	***	***	6.014
5.2.....	***	***	***	3.413	1.863	0.786	0.491	0.446	0.853	3.528	***	***	***	***	6.448
5.3.....	***	***	***	4.005	2.311	1.094	0.611	0.385	0.591	2.916	***	***	***	***	6.838
5.4.....	***	***	***	4.660	2.818	1.463	0.789	0.391	0.408	2.379	4.461	***	***	***	7.164
5.5.....	***	***	***	***	3.387	1.891	1.022	0.451	0.280	1.889	3.602	***	***	***	7.429
5.6.....	***	***	***	***	4.016	2.375	1.304	0.559	0.199	1.441	2.791	4.121	***	***	7.651
5.7.....	***	***	***	***	4.698	2.908	1.637	0.715	0.164	1.056	2.049	3.089	4.236	***	7.866
5.8.....	***	***	***	***	***	3.506	2.032	0.932	0.190	0.745	1.400	2.150	3.022	4.639	8.148
5.9.....	***	***	***	***	***	4.207	2.534	1.253	0.321	0.557	0.888	1.347	1.945	3.206	8.658
6.0.....	***	***	***	***	***	***	3.227	1.765	0.646	0.583	0.616	0.785	1.108	2.024	9.586
6.1.....	***	***	***	***	***	***	4.196	2.556	1.252	0.910	0.666	0.559	0.613	1.200	10.794
6.2.....	***	***	***	***	***	***	***	3.652	2.168	1.567	1.063	0.690	0.485	0.747	12.146
6.3.....	***	***	***	***	***	***	***	***	3.470	2.628	1.881	1.256	0.801	0.762	13.959
6.4.....	***	***	***	***	***	***	***	***	***	4.050	3.076	2.215	1.522	1.200	15.218
6.5.....	***	***	***	***	***	***	***	***	***	***	4.383	3.304	2.382	1.795	15.727
6.6.....	***	***	***	***	***	***	***	***	***	***	***	4.393	3.255	2.420	16.024
6.7.....	***	***	***	***	***	***	***	***	***	***	***	***	4.129	3.061	16.353
6.9.....	***	***	***	***	***	***	***	***	***	***	***	***	***	4.579	17.855

ionization, and a lower κ usually increases the mean charge. However, above 10^6 K, and at the high-temperature end of a transition between plateaux, DR can have particularly high resonance energies, and the enhanced suprathermal electron tail for lower κ can increase the overall recombination rate and lead to a decrease in the mean charge.

Returning to a description of the results, in general the equilibrium ionization fractions and mean charge change rapidly with temperature when the thermal energy is close to the threshold ionization energy of an atomic shell. Thus, the effect of a kappa distribution is particularly important at temperatures where the ion can lose electrons easily, i.e., not at a closed shell. Due to shell effects, for various elements and T values we observe more than one local maximum in the ionization fraction versus q.

At low temperatures, a lower value of κ (i.e., a more enhanced suprathermal tail in the electron distribution, with a harder power law) leads to a dominant ionization fraction at higher q, and a higher mean charge, $\langle Q \rangle$. While the thermal energy, $k_B T$, is less than the ionization threshold energy, the ionization processes take place more frequently due to the enhanced numbers of high-energy electrons.

Similarly, when the temperature is below the ionization threshold for a deeper shell, at the beginning of a transition from one closed shell plateau to another, a lower κ value again increases the mean charge. These effects of increasing mean charge have been pointed out in previous studies.

However, sometimes a lower κ value can lead to a lower $\langle Q \rangle$ (see Fig. 2), for $T > 10^6$ K and at the high-temperature end of a transition between plateaux. This effect has not been discussed previously (to our knowledge), but it can also be seen from the graphs of Ko et al. (1996). In addition, we have confirmed that this effect is present in results for Fe by Dzifčáková (1992), when the mean charge is computed from her tabulated ionization fractions.

Why does a lower κ reduce the mean charge only in temperature ranges where $\langle Q \rangle$ is approaching a closed-shell plateau? A physical explanation is that for ionization to a closed shell, say, the K shell, there is a competition between ionization of the last L-shell electron, with a relatively low threshold, and recombination to capture an electron into the L shell. Dielectronic recombination (DR) requires a particularly high energy, because it involves excitation of a K-shell electron. Referring to the discussion earlier in this section, we are in the "low-temperature" régime, where $k_B T$ is less than the threshold/resonance energies in question. Indeed, that is what defines the temperature range of the transition between plateaux: the temperature is not yet high enough to completely strip the higher shell electrons, let alone the deeper shell electrons. Therefore, for lower κ and a stronger high-energy tail, the DR (and overall recombination) rate increases and $\langle Q \rangle$ is reduced.

Considering $\langle Q \rangle$ as a function of temperature, the approach to a new closed-shell plateau is more gradual for lower κ. On the other hand, at the start of a transition from one plateau to another, a lower κ increases $\langle Q \rangle$ because of enhanced ionization; therefore, the overall effect is that a lower κ value leads to broader transitions from one closed-shell plateau to another, as can be seen in Figures 2–4.

TABLE 3B

IONIZATION FRACTIONS FOR Fe AS A FUNCTION OF TEMPERATURE FOR A KAPPA DISTRIBUTION OF ELECTRON VELOCITY, WITH $\kappa = 5$: Fe^{+13}–Fe^{+26}

log T	Fe^{+13}	Fe^{+14}	Fe^{+15}	Fe^{+16}	Fe^{+17}	Fe^{+18}	Fe^{+29}	Fe^{+20}	Fe^{+21}	Fe^{+22}	Fe^{+23}	Fe^{+24}	Fe^{+25}	Fe^{+26}	$\langle Q \rangle$
5.8.....	4.639	***	***	***	***	***	***	***	***	***	***	***	***	***	8.148
5.9.....	3.206	4.530	***	***	***	***	***	***	***	***	***	***	***	***	8.658
6.0.....	2.024	2.987	4.154	4.593	***	***	***	***	***	***	***	***	***	***	9.586
6.1.....	1.200	1.814	2.603	2.772	4.652	***	***	***	***	***	***	***	***	***	10.794
6.2.....	0.747	1.025	1.461	1.412	2.981	***	***	***	***	***	***	***	***	***	12.146
6.3.....	0.762	0.721	0.833	0.606	1.893	3.685	***	***	***	***	***	***	***	***	13.959
6.4.....	1.200	0.859	0.678	0.299	1.329	2.763	4.202	***	***	***	***	***	***	***	15.218
6.5.....	1.795	1.172	0.728	0.209	1.004	2.114	3.210	4.695	***	***	***	***	***	***	15.727
6.6.....	2.420	1.534	0.855	0.203	0.770	1.584	2.368	3.535	4.882	***	***	***	***	***	16.024
6.7.....	3.061	1.930	1.040	0.257	0.610	1.148	1.639	2.517	3.554	4.800	***	***	***	***	16.353
6.8.....	3.754	2.396	1.313	0.400	0.546	0.827	1.051	1.658	2.408	3.343	4.489	***	***	***	16.902
6.9.....	4.579	3.010	1.748	0.704	0.645	0.686	0.665	1.020	1.506	2.153	3.009	4.038	***	***	17.855
7.0.....	***	3.843	2.414	1.239	0.985	0.799	0.555	0.676	0.918	1.299	1.891	2.647	***	***	19.111
7.1.....	***	4.943	3.355	2.049	1.603	1.202	0.736	0.634	0.646	0.784	1.131	1.642	4.271	***	20.446
7.2.....	***	***	4.533	3.095	2.463	1.858	1.188	0.875	0.672	0.574	0.698	0.986	3.230	***	21.657
7.3.....	***	***	***	4.302	3.494	2.694	1.831	1.318	0.912	0.600	0.511	0.603	2.490	4.876	22.544
7.4.....	***	***	***	***	4.600	3.616	2.572	1.869	1.271	0.757	0.473	0.390	1.944	3.984	23.095
7.5.....	***	***	***	***	***	4.560	3.343	2.459	1.681	0.977	0.511	0.275	1.526	3.246	23.433
7.6.....	***	***	***	***	***	***	4.111	3.056	2.106	1.226	0.592	0.216	1.186	2.609	23.668
7.7.....	***	***	***	***	***	***	4.869	3.650	2.537	1.489	0.700	0.199	0.910	2.065	23.866
7.8.....	***	***	***	***	***	***	***	4.241	2.973	1.769	0.833	0.217	0.693	1.599	24.069
7.9.....	***	***	***	***	***	***	***	4.834	3.417	2.065	0.994	0.270	0.534	1.219	24.293
8.0.....	***	***	***	***	***	***	***	***	3.871	2.381	1.185	0.360	0.430	0.912	24.542
8.1.....	***	***	***	***	***	***	***	***	4.339	2.718	1.407	0.486	0.376	0.676	24.799
8.2.....	***	***	***	***	***	***	***	***	4.812	3.069	1.651	0.638	0.365	0.501	25.038
8.3.....	***	***	***	***	***	***	***	***	***	3.426	1.908	0.810	0.388	0.374	25.242
8.4.....	***	***	***	***	***	***	***	***	***	3.778	2.169	0.989	0.431	0.284	25.403
8.5.....	***	***	***	***	***	***	***	***	***	4.118	2.425	1.169	0.488	0.219	25.528
8.6.....	***	***	***	***	***	***	***	***	***	4.449	2.677	1.347	0.552	0.172	25.623
8.7.....	***	***	***	***	***	***	***	***	***	4.761	2.917	1.518	0.618	0.138	25.695
8.8.....	***	***	***	***	***	***	***	***	***	***	3.142	1.679	0.684	0.113	25.749
8.9.....	***	***	***	***	***	***	***	***	***	***	3.355	1.833	0.749	0.093	25.791
9.0.....	***	***	***	***	***	***	***	***	***	***	3.555	1.977	0.812	0.078	25.824

In sum, taking into account a kappa distribution of electrons, which is apparently the norm rather than the exception in astrophysical plasmas, can substantially change the interpretation of ionization state measurements. For example, a measurement of the mean charge is often used to infer the plasma temperature, and that inference is greatly affected by the value of κ, as shown in Figures 2–4. The κ value also strongly affects the interpretation of measurements of dominant ionization states or ionization ratios (effects on the latter were described in detail by Owocki & Scudder 1983).

3.2. *Comparison with Other Calculations*

In this section, we discuss how our results compare with those of other authors. To our knowledge, results of ionization fractions for kappa distributions for multiple elements (besides Fe) have not been previously presented; however, we can compare our results with previous calculations of ionization fractions for Maxwellian distributions (Mazzotta et al. 1998), ionization fractions for kappa distributions in the case of Fe (Dzifčáková 1992), and mean charges for kappa distributions for C, N, O, Ne, Mg, Si, and S (Luhn & Hovestadt 1985) and for C, O, Mg, Si, and Fe (Ko et al. 1996).

Some of these results are compared graphically in Figures 3 and 4, for the restricted temperature range of 10^5 to 10^8 K. (Note that the Fe results of Arnaud & Raymond 1992 would be indistinguishable from those of Mazzotta et al. 1998; thus, they are not shown in Fig. 4*a*.) We find qualitative agreement in all cases. Quantitative differences are ascribed to different cross section assumptions; thus, the comparison with other work gives an indication of the uncertainty in any given calculation. In general, the discrepancies between different calculations are greater for heavier elements.

We have compared our results for the case of Maxwellian distribution with those of Mazzotta et al. (1998). Indeed, we should expect good agreement because we have used similar ionization and recombination cross sections, with some exceptions as noted in § 2. For N through S ions, our $\langle Q \rangle$ values never differ from those derived from ionization fractions of Mazzotta et al. (1998) by more than 0.2. Differences greater than 0.1 only appear at a few temperature ranges where $\langle Q \rangle$ is rapidly varying with temperature. For heavier ions the differences are greater, especially where $\langle Q \rangle$ rapidly varies with temperature, but are never greater than half of a charge unit.

Ionization fractions for Fe have been calculated by Dzifčáková (1992), assuming both Maxwellian and kappa distributions for the electron velocity. We find major differences between those results and ours, even for a Maxwellian distribution. For example, when we evaluate the mean charge based on the ionization fractions presented by Dzifčáková (1992), we find that it differs from ours by $\approx$1 for multiple temperature ranges, even in ranges where our results are very similar to those of Mazzotta

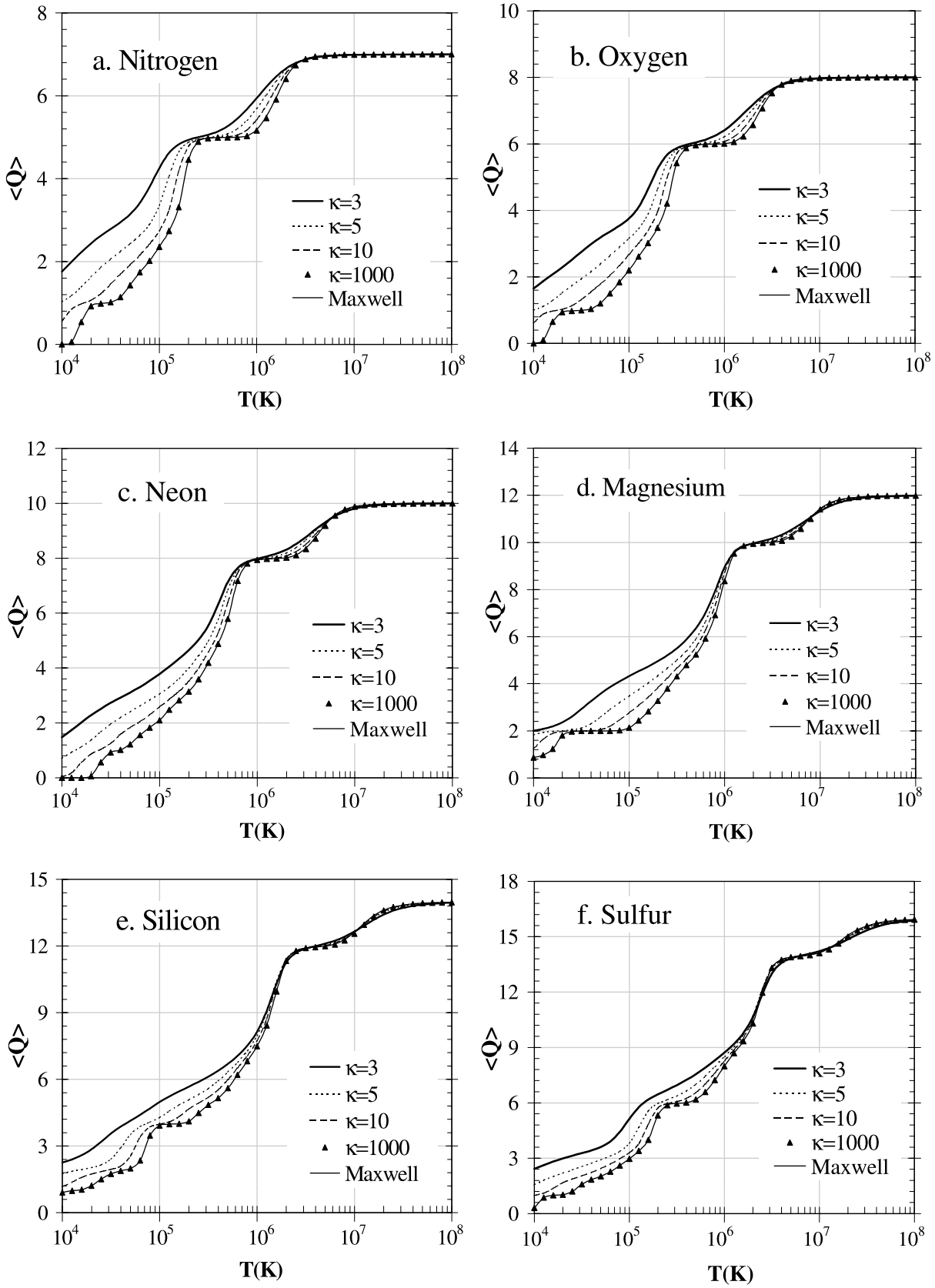

FIG. 2.—Mean equilibrium charge, $\langle Q \rangle$, as a function of electron temperature for (*a*) nitrogen, (*b*) oxygen, (*c*) neon, (*d*) magnesium, (*e*) silicon, (*f*) sulfur, (*g*) argon, (*h*) calcium, (*i*) iron, and (*j*) nickel.

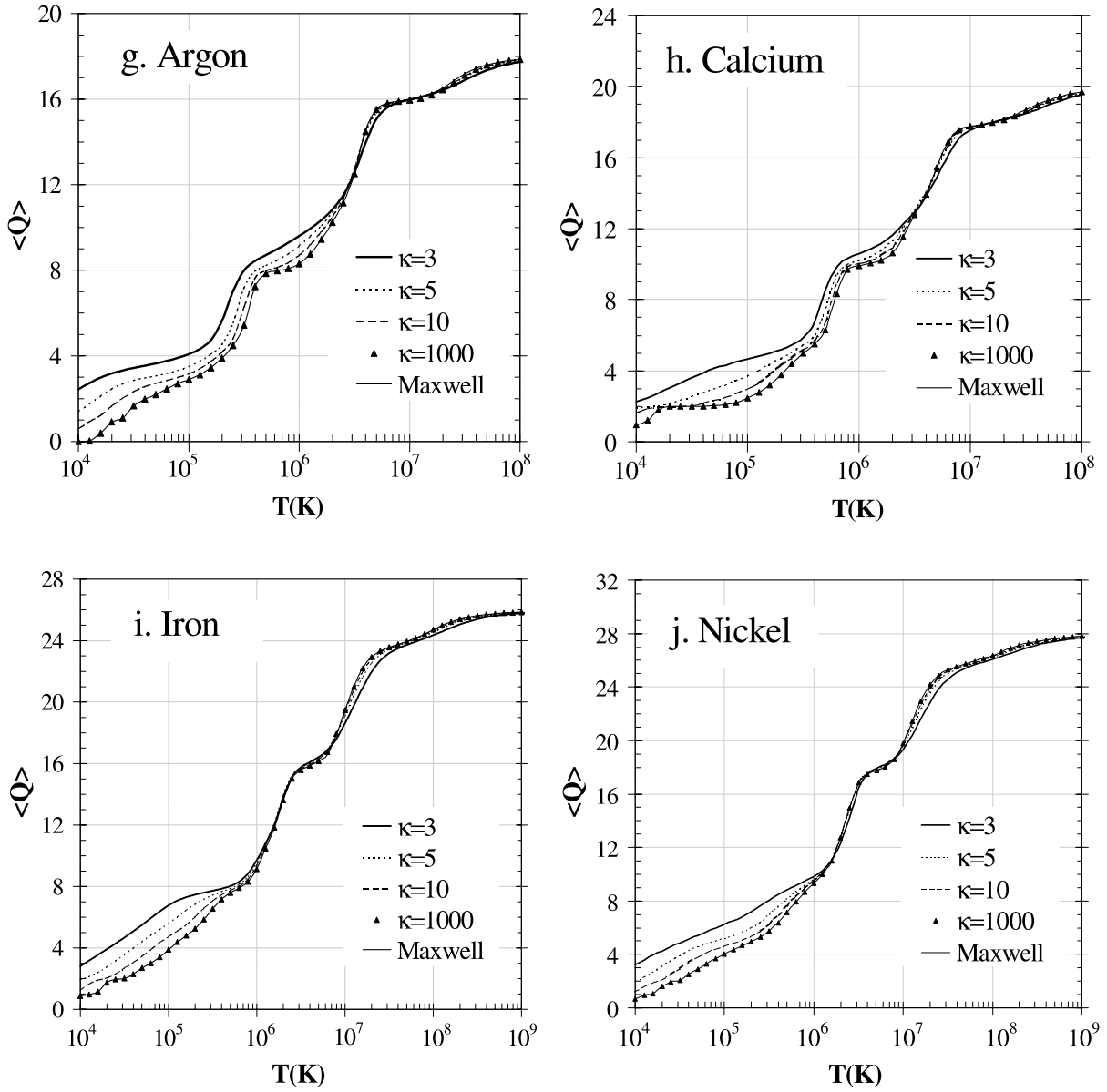

FIG. 2.—*Continued*

et al. (1998). We attribute this to the use of different ionization and recombination cross sections; for example, Dzifčáková (1992) used ionization cross sections from Arnaud & Rothenflug (1985), whereas Mazzotta et al. (1998) and our work have used ionization cross sections from Arnaud & Raymond (1992). Indeed, later work by Dzifčáková (1998) for the case of a Maxwellian distribution implies mean charges much closer to those of Mazzotta et al. (1998) and our work (the difference is frequently not visible in Fig. 4*a*). However, at temperatures above 10^7 K, the ionization fractions of Dzifčáková (1992, 1998) imply that the mean charge oscillates with temperature, which was not found by Mazzotta et al. (1998) or our own work.

Regarding the effects of a kappa distribution, we have compared our mean charges with those obtained from ionization fractions presented by Dzifčáková (1992) for Fe and from figures presented by Luhn & Hovestadt (1985) and Ko et al. (1996) for various elements (Figs. 3 and 4). The effects described in § 3.1 are qualitatively confirmed in each case. There are some quantitative differences, presumably related to the choice of cross sections. In the case of heavier elements, Si and Fe, in transition regions our results show less variation with the κ value than those of Ko et al. (1996).

4. CONCLUSIONS

The ionization fractions for various elements (N, O, Ne, Mg, Si, S, Ar, Ca, Fe, and Ni) are calculated with consideration of electron distributions similar to those observed in actual space plasmas, which have pronounced suprathermal, power-law tails, here modeled by the kappa distribution. A subset of our results can be compared with previous results by other authors, with minor differences attributed to the use of different cross section formulae. In particular, we have confirmed that our calculation results in the limit of a Maxwellian distribution are very similar to the previous results of Mazzotta et al. (1998).

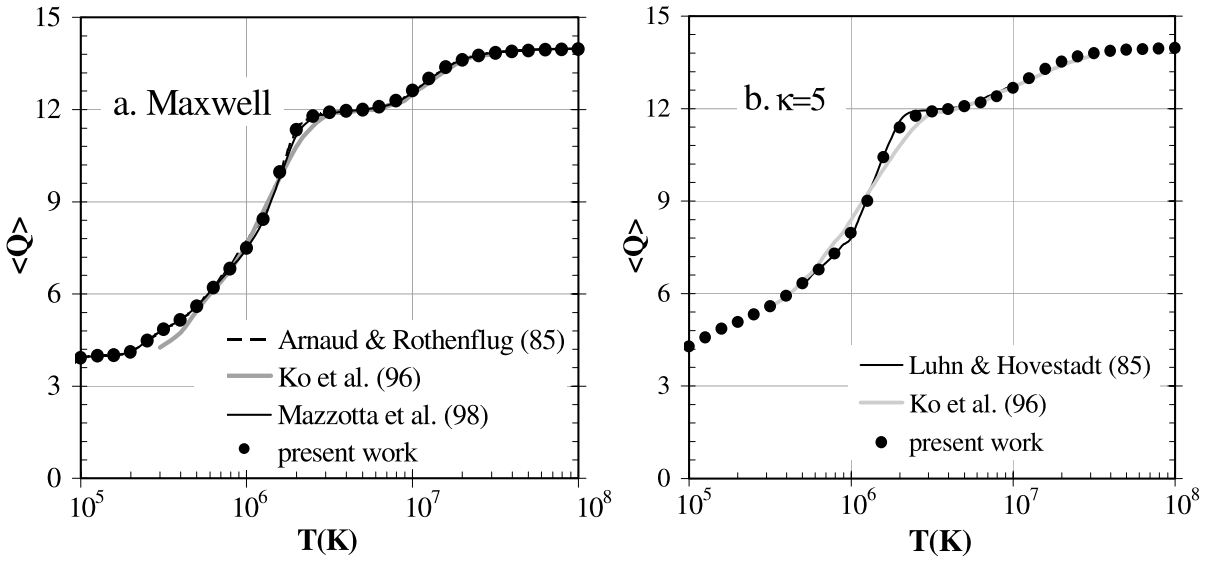

FIG. 3.—Comparison among various results for $\langle Q \rangle$ vs. T, for Si

We found that the effect of the enhanced high-energy tail, as parameterized by the κ value, depends sensitively on the plasma temperature. The most dramatic effect is that at low temperature, a lower κ value shifts the ionization balance toward a higher charge. Otherwise, the κ value mainly affects ionization fractions when the thermal energy is close to the ionization threshold for valence electrons, and the mean charge as a function of temperature undergoes a transition from one closed shell plateau to another. We point out that at the upper end of such a transition range, a lower κ (and stronger high-energy tail) actually decreases the mean charge, which in retrospect can also be seen in the previous results of Ko et al. (1996) and in mean charges calculated from the tabulated ionization fractions of Dzifčáková (1992). This results from the κ dependence of ionization and recombination rates; we found that κ strongly affects the temperature dependence of ionization or dielectronic recombination rates for which the corresponding cross sections have sharp energy thresholds or resonance conditions, respectively. The overall effect is that a lower κ leads to broader transitions in mean charge as a function of temperature, from one closed shell to another.

Therefore, in many types of astrophysical situations, it is impossible to avoid the effect of an enhanced number of high-energy electrons on the ionization balance of various elements. This in turn affects the interpretation of a wide variety of astrophysical observations, where observed ionization fractions or the presence of a given ion serves as a diagnostic of the plasma temperature. The tables presented here and at our Web site[2] may be useful in the interpretation of such observations.

[2] The tables are also available at http://www.sc.chula.ac.th/kappa.

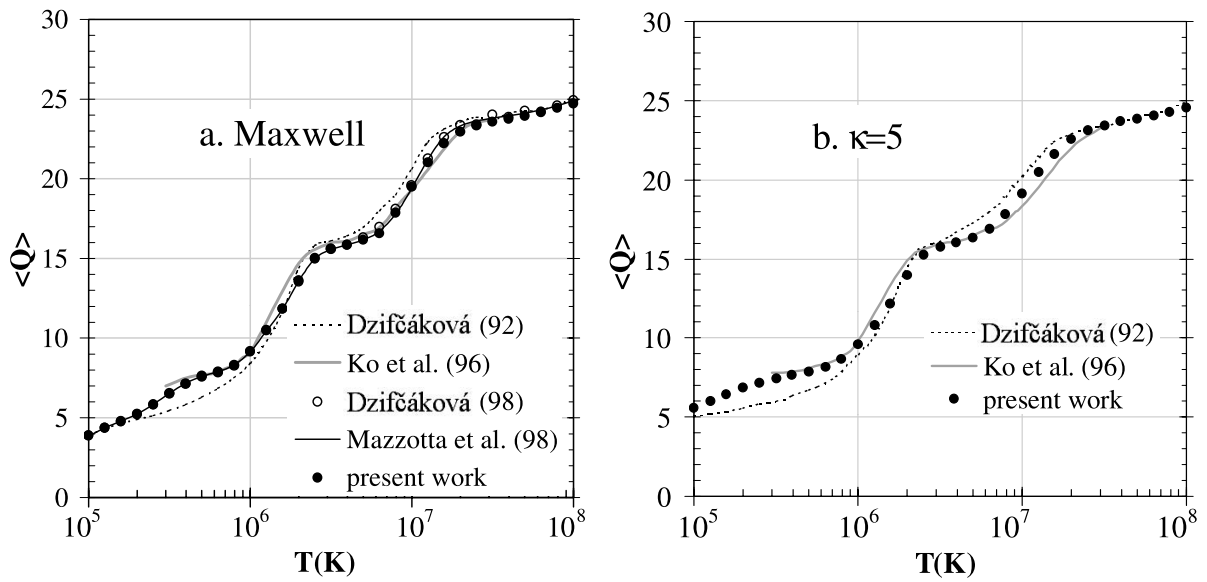

FIG. 4.—Comparison among various results for $\langle Q \rangle$ vs. T, for Fe

The authors are grateful to Stan Owocki for helpful discussions and to an anonymous referee for useful suggestions. We thank Phantip Hosesomephan for her assistance with tables. This research was partially supported by a Basic Research Grant from the Thailand Research Fund, NASA grant NAG 5-8134, and by the Russian Foundation of Basic Research, grant 00-02-17031.

REFERENCES

Arnaud, M., & Raymond, J. 1992, ApJ, 398, 394
Arnaud, M., & Rothenflug, R. 1985, A&AS, 60, 425
Blair, W. P., et al. 2000, ApJ, 538, L61
Brosius, J. W. 2001, ApJ, 555, 435
Collier, M. R. 1999, J. Geophys. Res., 104, 28559
Danforth, C., Blair, W. P., & Raymond, J. C. 2001, ApJ, 122, 938
Drake, J. J., Brickhouse, N. S., Kashyap, V., Laming, J. M., Huenemoerder, D. P., Smith, R., & Wargelin, B. J. 2001, ApJ, 548, L81
Dzifčáková, E. 1992, Sol. Phys., 140, 247
———. 1998, Sol. Phys., 178, 317
Esser, R., & Edgar, R. 2000, ApJ, 532, L71
Fang, T., & Canizares, C. R. 2000, ApJ, 539, 532
Fang, T., Marshall, H. L., Bryan, G. L., & Canizares, C. R. 2001, ApJ, 555, 356
Feldman, W. C., Asbridge, J. R., Bame, S. J., Montgomery M. D., & Gary S. P. 1975, J. Geophys. Res., 80, 4181
Gallagher, P. T., Phillips, K. J. H., Lee, J., Keenan, F. P., & Pinfield, D. J. 2001, ApJ, 558, 411
Gloeckler, G., et al. 1999, Geophys. Res. Lett., 26, 157
Hasegawa, A., Mima, K., & Duong-van, M. 1985, Phys. Rev. Lett., 54, 2608
Hicks, A. K., & Canizares, C. R. 2001, ApJ, 556, 468
Huenemoerder, D. P., Canizares, C. R., & Schulz, N. S. 2001, ApJ, 559, 1135
Kartavykh, Yu. Yu., Wannawichian, S., Ruffolo, D., & Ostryakov, V. M. 2002, Adv. Space Res., 30(1), 119
Ko, Y.-K., Fisk, L., Gloeckler, G., & Geiss, J. 1996, Geophys. Res. Lett., 23, 2785
Kocharov, L., Kovaltsov, G. A., Torsti, J., & Ostryakov, V. M. 2000, A&A, 357, 716
Luhn, A., & Hovestadt, D. 1985, in 19th Int. Cosmic-Ray Conf. (La Jolla), ed. F. C. Jones, J. Adams, & G. M. Mason (Washington: NASA), 245
———. 1987, ApJ, 317, 852
Ma, C.-Y., & Summers, D. 1998, Geophys. Res. Lett., 25, 4099
———. 1999a, Geophys. Res. Lett., 26, 181
Ma, C.-Y., & Summers, D. 1999b, Geophys. Res. Lett., 26, 1121
Maksimovic, M., Pierrard, V., & Riley, P. 1997, Geophys. Res. Lett., 24, 1151
May, M. J., et al. 2000, ApJ, 61, 3042
Mazzotta, P., Mazzitelli, G., Colafrancesco, S., & Vittorio, N. 1998, A&AS, 133, 403
Möbius, E., et al. 1999, Geophys. Res. Lett., 26, 145
Montgomery, M., Bame S. J., & Hundhausen A. J. 1968, J. Geophys. Res., 73, 4999
Olbert, S. 1969, in Physics of Magnetospheres, ed. R. C. Carovillano, J. F. McClay, & H. R. Radoski (Boston: Reidel), 19
Olbert, S., Egidi A., Moreno, G., & Pai, L., G. 1967, Eos Trans. AGU, 48, 177
Owocki, S. P., & Canfield, R. C. 1986, ApJ, 300, 420
Owocki, S. P., & Scudder, J. D. 1983, ApJ, 270, 758
Ostryakov, V. M., Kartavykh, Y. Y., Ruffolo, D., Kovaltsov, G. A., & Kocharov, L. 2000, J. Geophys. Res., 105, 27315
Pierrard, V., Maksimovic, M., & Lemaire, J. 1999, J. Geophys. Res., 104, 17021
Reynolds, C. S., Heinz, S., & Begelman, M. C. 2001, ApJ, 549, L179
Roussel-Dupré, R. 1980, Sol. Phys., 68, 243
Roussev, I., Doyle, J. G., Galsgaard, K., & Erdélyi, R. 2001, A&A, 380, 719
Sampson, D. H., & Golden, L. B. 1981, J. Phys. B, 14, 903
Scudder, J. D., & Olbert, S. 1979a, J. Geophys. Res., 84, 2755
———. 1979b, J. Geophys. Res., 84, 6603
Shoub, E. C. 1983, ApJ, 266, 339
Shull, J. M., & Van Steenberg, M. 1982a, ApJS, 48, 95
———. 1982b, ApJS, 49, 351
Smith, R. K., Brickhouse, N. S., Liedahl, D. A., & Raymond, J. C. 2001, ApJ, 556, L91
Verner, D. A., & Ferland, G. J. 1996, ApJS, 103, 487
Voronov, G. S. 1997, At. Data Nucl. Data Tables, 65, 1
Wu, K., Cropper, M., & Ramsay, G. 2001, MNRAS, 327, 208
Younger, S. M. 1981, Phys. Rev. A, 24, 1272